Dynamics of $I^*(^2P_{1/2})$ production in the ultraviolet photodissociation of alkyl iodides

S. Uma and Puspendu Kumar Das[1]

Department of Inorganic and Physical Chemistry, Indian Institute of Science, Bangalore 560 012, India

Received July 5, 1993

This paper is dedicated to Professor John C. Polanyi on the occasion of his 65th birthday

S. Uma and Puspendu Kumar Das. Can. J. Chem. **72**, 865 (1994).

The relative quantum yields, ϕ^*, for the production of $I^*(^2P_{1/2})$ at 266, 280, and ~305 nm are reported for a series of primary alkyl iodides using the technique of two-photon laser-induced fluorescence for the detection of $I(^2P_{3/2})$ and $I^*(^2P_{1/2})$ atoms. Results are analyzed by invoking the impulsive energy disposal model, which summarizes the dynamics of dissociation as a single parameter. Comparison of our data with those calculated by a more sophisticated time-dependent quantum mechanical model is also made. Near the red edge of the alkyl iodide *A* band, absorption contribution from the $^3Q_1$ state is important and the dynamics near the $^3Q_0$–$^1Q_1$ curve-crossing region seem to be influenced by the kinematics of the dissociation process.

S. Uma et Puspendu Kumar Das. Can. J. Chem. **72**, 865 (1994).

On a déterminé les rendements quantiques relatifs, ϕ^*, pour la production de $I^*(^2P_{1/2})$ à 266, 280 et environ 305 nm, pour une série d'iodures d'alkyles primaires; pour ce faire, on a utilisé la technique de fluorescence à deux photons induite au laser pour la détection des atomes de $I(^2P_{3/2})$ et de $I^*(^2P_{1/2})$. On a analysé les résultats en invoquant le modèle de disposition de l'énergie impulsive qui résume les dynamiques de dissociation en un seul paramètre. On a effectué une comparaison de nos résultats avec ceux calculés à l'aide d'un modèle plus sophistiqué de mécanique quantique dépendant du temps. Au niveau de la limite du rouge de l'absorption de la bande *A* de l'iodure d'alkyle, la contribution de l'état $^3Q_1$ est importante et la dynamique près de la région du croisement de la courbe $^3Q_0$–$^1Q_1$ semble être influencée par la cinématique du processus de dissociation.

[Traduit par la rédaction]

Introduction

Photodissociation dynamics of simple alkyl iodides in the *A* band arising from $n \rightarrow \sigma^*$ ($X \rightarrow A$) transition has been of interest over the last two decades. This is mainly because alkyl iodides offer an unique opportunity to understand key factors such as radical size (CH_3, C_2H_5, C_3H_7, etc.), substitution (CH_3, CF_3, etc.), and structure (primary, secondary, and tertiary) that affect their photodissociation dynamics. Subsequent to the measurement of magnetic circular dichroism (MCD) spectra of CH_3I by Gedanken and Rowe (1), several groups (2–16) came up with a variety of techniques to investigate the dynamics of alkyl iodide photodissociation. Riley and Wilson (2) and Dzvonik et al. (3) simultaneously carried out photodissociation experiments on CH_3I using the time-of-flight (TOF) technique. From the results, they concluded that at 260 nm the transition dipole is predominantly parallel to the C—I bond ($^3Q_0 \leftarrow {}^1A_1$) and the dissociation leads to $I(^2P_{1/2})$ (will be called I* from now) and $CH_3^{\cdot}$ radicals as major products. Later Sparks et al. (4) carried out another TOF experiment on CH_3I at 266 nm; they extracted the ν_2 (umbrella mode of CH_3) vibrational distribution of CH_3 fragments from the spectrum and found that it peaked at $v = 2$. Hermann and Leone (5) measured the infrared emission from CH_3 radicals produced from CH_3I at 248 and 266 nm. Their results at 266 nm agreed well with those of Sparks et al. (4). At 248 nm the vibrational distribution was again found to peak at $v = 2$, which differed from the theoretical results of Shapiro and Bersohn (6) who had predicted the product distribution maximum at $v = 4$ at that wavelength. In 1984, a new TOF experiment on methyl iodide at 248 nm was carried out by van Veen et al. (7). They found two peaks in the spectrum corresponding to $I(^2P_{3/2})$ (will be called I from now) and I* products and both the convoluted vibrational distributions peaked at $v = 2$. Brewer et al. (8) measured the quantum yield of I* production for a series of alkyl iodides at 248 nm using a two-photon laser-induced fluorescence (TPLIF) detection scheme for both I and I* atoms. Photofragmentation of CH_3I at 248 nm was studied by Barry and Gorry (9); they observed the ν_2 vibrational distribution to peak at $v = 2$ for the I* channel, and to extend up to $v = 8$ for the I channel. Using the TPLIF technique, Godwin et al. (10) measured the quantum yield for production of I and I* for a series of alkyl iodides at 248 nm. They observed that the I* yield or the dynamics of I* production varies with the alkyl radical size, substitutions on α- and β-carbon atoms, and structure. Using a diode laser to probe the dissociation dynamics of CH_3I at 266 nm, Hess et al. (11) measured the I* quantum yield as 0.73 ± 0.04. At 229.4 nm Penn et al. (12) also found that I* is the major product from CH_3I. In 1989 Ogorzalek Loo et al. (13) looked again at the vibrational distribution of CH_3 at 266 nm using the multiphoton ionization technique for detecting CH_3 fragments in their vibrational states. They predicted that $v = 0$ is the most populated umbrella vibration in CH_3 fragments, in disagreement with the results obtained by Sparks et al. (4). The authors (13) ascribed the difference to contamination by vibrationally excited CH_3I in the latter experiment. The I* yield increases with increasing vibrational excitation in the methyl fragment and the estimated net yield is 0.56, which is lower than the value measured by other direct techniques.

In this work we report ϕ^*, the relative quantum yield for I* production (i.e., $\phi^* = [I^*]/([I] + [I^*])$), for a series of simple alkyl iodides at three different dissociation wavelengths: 266, 280, and ≃305 nm. The resulting atomic fragments $I(^2P_{3/2})$ and $I^*(^2P_{1/2})$ have been probed directly using the TPLIF technique (8). At ≃305 nm I and I* atoms were produced by the same pulse that was used for probing. From now on the experiments at 266 and 280 nm wavelengths will be referred to as pump–probe experiments and that at ≃305 nm as a single laser experiment. We discuss our results in the light of a classical Landau–Zener model and compare them with recent theoretical and experimental results obtained by other groups.

[1]Author to whom correspondence may be addressed. FAX: 91-080-3341683.

TABLE 1. Relative quantum yield (ϕ^*) of I* production at different dissociation wavelengths

Molecule	ϕ^* ≃305 nm	ϕ^* 280 nm	ϕ^* 266 nm
Methyl iodide	0.43 ± 0.01	0.69 ± 0.02	0.79 ± 0.02
Ethyl iodide	0.39 ± 0.02	0.60 ± 0.02	0.73 ± 0.02
n-Propyl iodide	0.35 ± 0.02	0.56 ± 0.02	0.66 ± 0.02
n-Butyl iodide	0.30 ± 0.02	0.50 ± 0.03	0.64 ± 0.03
Isobutyl iodide	0.35 ± 0.02	0.56 ± 0.03	0.71 ± 0.01

Experimental setup

The apparatus used in our experiments has been described in detail elsewhere (17). Briefly, a sample gas is contained at 50–70 mTorr (1 Torr = 133.3 Pa) in a stainless steel cell that is pumped continuously by a diffusion pump and the pressure monitored by an MKS Baratron gauge (model 122A). The pump and the probe lasers are crossed perpendicular inside the chamber and the signal is detected at the third perpendicular direction. The fourth harmonic of a Nd-YAG laser (DCR-3G, Spectra Physics) was used for dissociation at 266 nm (≃19 mJ/pulse) whereas the second harmonic of a Nd:YAG pumped dye laser was employed for the photolysis experiments at 280 nm (≃5 mJ/pulse). A typical delay of 400 ns between the pump and the probe lasers was maintained to avoid collisional relaxation of the nascent fragments. The resulting iodine atoms were detected by the technique of TPLIF using another doubled dye laser ("probe" laser) output (≃0.5 mJ/pulse). In the case of ≃305 nm dissociation, the probe laser alone was used but with tight focussing by a 5-in. focal length Suprasil lens at the center of the cell. The VUV fluorescence was detected through a MgF_2 window by a solar blind PMT (Thorn EMI, model 9423B). The space between the window and the PMT was continuously flushed with dry nitrogen. The signal was amplified (×25) by a preamplifier (SRS 440) and averaged in a gated boxcar averager (SRS 250), the output of which was fed to a strip-chart recorder for display. The alkyl iodides were obtained commercially or prepared by standard procedures. All the iodides were decolorized with 10% sodium bisulfite solution, dried on anhydrous $MgSO_4$, and fractionally distilled prior to each experiment.

Results

The VUV emission spectra were recorded by scanning the probe laser across the two-photon absorption lines of I (304.7 nm) and I* (306.7 nm). Typical TPLIF spectra of I* and I are shown in Fig. 1. The relative quantum yield, ϕ^*, was determined directly from the spectra. Here we took the experimental signal intensities S and S^* as being directly proportional to [I] and [I*], respectively. Since our ϕ^* value of 0.79 for CH_3I at 266 nm agrees very well with the same (0.76) found by Riley and Wilson (2) by photofragment spectroscopy, no calibration was done to our raw data.

The quantum yields for I* production obtained at three different wavelengths are listed in Table 1. For the pump–probe experiments, the signal varies linearly with the pump laser power (Fig. 2*a*). For all pump–probe experiments care was taken to reduce the probe-alone contribution to ≤2%. In the single laser experiment the very small difference in the absorption coefficients at 304.7 and 306.7nm is neglected. A power dependence study shows that three photons are involved in the process (Fig. 2*b*), implying that one photon is utilized for the dissociation and two subsequent photons for probing the iodine fragments.

Discussion

The *A* band in the absorption of alkyl iodides arising from a

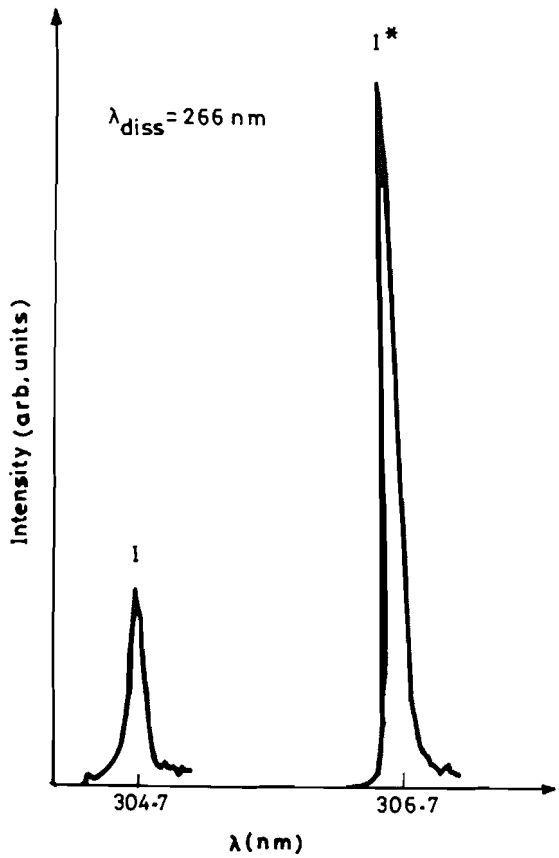

FIG. 1. Typical TPLIF spectra of I and I* from CH_3I dissociation at 266 nm.

$n \rightarrow \sigma^*$ transition is strongly localized on the C—I bond. Gedanken and Rowe (1) resolved that *A* band using MCD. The three possible transitions are labelled according to Mulliken (18) as $^1Q_1 \leftarrow N$, $^3Q_1 \leftarrow N$, and $^3Q_0 \leftarrow N$. The first two transitions are perpendicular transitions leading to the formation of I, whereas the third is a parallel transition that leads to I*. Figure 3 displays a schematic one-dimensional potential energy diagram showing all these states. The electronic transition at 266 and 280 nm is mainly to the $^3Q_0$ state but a significant amount of I atoms (Table 1) are produced by a curve-crossing mechanism from $^3Q_0$ to $^1Q_1$. At these wavelengths no significant contribution is made by the $^3Q_1$ state, as pointed out by Gedanken and Rowe (1). The energy disposal at these two wavelengths may be best described by a simple classical model suggested by Godwin et al. (10). In their model the I* quantum yield is described by the probability of staying on the initial $^3Q_0$ state as,

$$[1] \quad \phi^* = \exp(-2\pi V_{12}^2/\hbar|\Delta F|v) = \exp(-\zeta/v)$$

where V_{12} is the coupling term between the $^3Q_0$ and $^1Q_1$ states, ΔF is the difference in their gradients at the crossing point, and v is the velocity through the crossing point. Further, they grouped the unknowns V_{12} and ΔF into one parameter to determine if it remains the same for a series of related alkanes. Hence the problem is simplified to the extent of finding the velocity at the crossing point. For this the translational energy (E_t) at the asymptotic limits is calculated using a quasidiatomic model and is given by

$$[2] \quad E_t = (\mu_{Cl}/\mu_{RI})E_{avl}$$

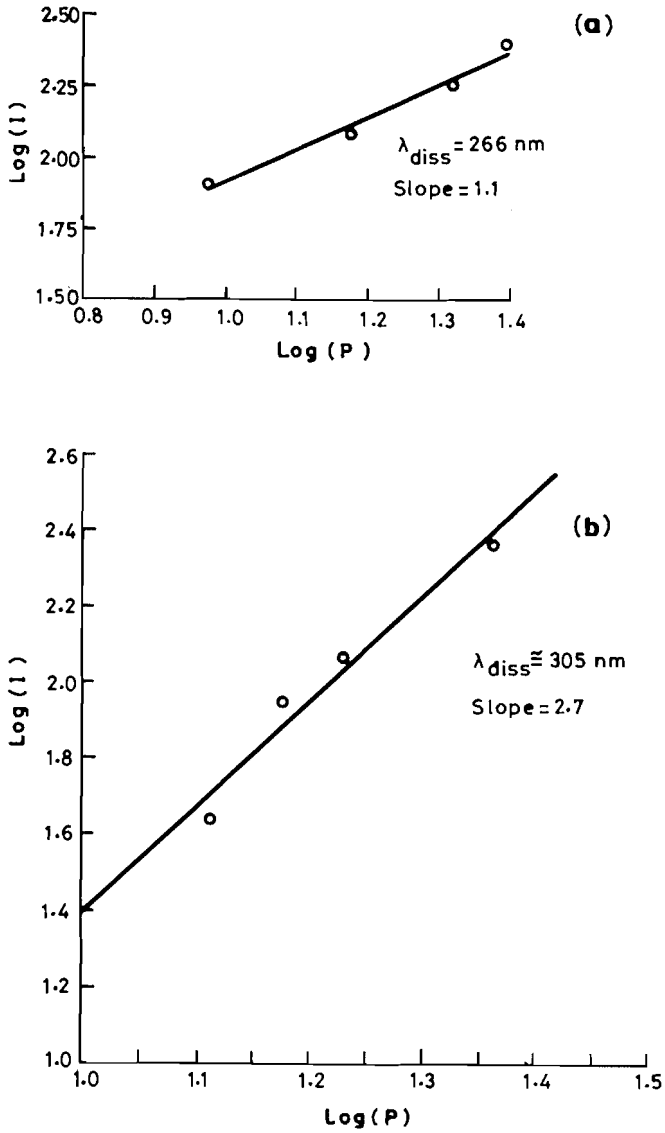

FIG. 2. (*a*) A log–log plot of the pump laser (266 nm) power and the iodine atom signal intensity for the pump–probe experiment. (*b*) A log–log plot of the probe laser power and the iodine atom signal intensity for the single laser experiment. The slope gives the laser power dependence of the signal in each case.

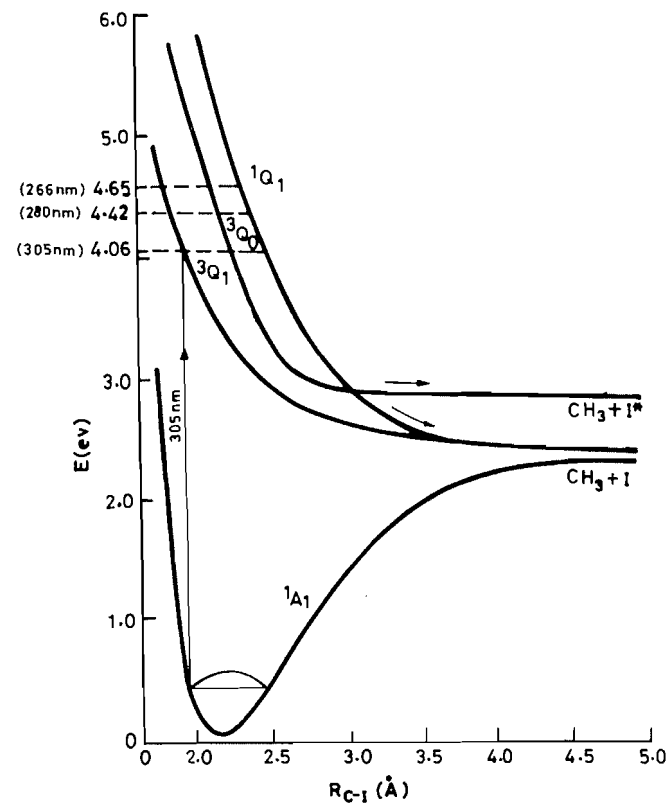

FIG. 3. Schematic potential energy surfaces for the alkyl iodides showing only the important states.

where μ_{CI} is the reduced mass of C and I, μ_{RI} the reduced mass of the radicals R and I, and E_{avl} is the available energy, which is $h\nu - D_0^0 - E_{so}$ with ν being the excitation frequency, D_0^0 the dissociation energy of the C—I bond at 0 K, and E_{so} is the iodine spin-orbit excitation energy. Now E_t must be linearly related to the translational energy at the crossing point and the proportionality constant, if any, may again be absorbed within the parameter ζ. Thus the final expression for ϕ^* becomes,

$$[3] \quad \phi^* = \exp\left[-\mu_{RI}\zeta/(2\,\mu_{CI}\,E_{avl})^{1/2}\right]$$

We have used this model at 266 and 280 nm and find reasonable fits to the experimental points with ζ being 670 m/s and 970 m/s, respectively (Figs. 4*a* and 4*b*). It is worth noting that although a single parameter describes the dynamics on the upper potential energy surfaces, most of the actual information (i.e., the coupling between the potential energy surfaces and the C—I bond length at the crossing point) is actually hidden in this parameter, as pointed out by Lao et al. (14). However, a detailed model to describe the dynamics will be complicated and computationally demanding. Also the predictive power of all such calculations will rely on the accuracy of the potential energy surfaces used. The quantum yield of I* at ~305 nm was not treated in this manner since at this wavelength I is the major product, which cannot be explained on the basis of the initial excitation to the $^3Q_0$ state. But if we look carefully at the different components of the *A* band, this is not at all surprising. Similar to the mechanism proposed by Hwang and El-Sayed (19, 20) in the case of CF_3I dissociation, at this wavelength the initial absorption in alkyl iodides is not mainly confined to the $^3Q_0$ state. The low-energy $^3Q_1$ state carries a significant transition strength (since the total absorption cross section at this wavelength is very small) and produces mainly the ground state I product through a direct dissociation mechanism. Therefore, production of I atoms at this wavelength may be attributed to the direct dissociation from the $^3Q_1$ state as well as curve crossing between the $^3Q_0$ and $^1Q_1$ states. However, it is clear from Table 1 that the extent of these two mechanisms varies as one goes from methyl to isobutyl iodide.

The trend reversal in the ϕ^* values in going from *n*-butyl iodide to isobutyl iodide may be explained qualitatively by considering the increased inductive and hyperconjugative effects in the latter. Since the excitation is localized on the C—I bond, the electronic charge distribution around this bond is likely to affect the dynamical outcome. V_{12} is unlikely to change in the family of primary alkyl iodides since it is directly proportional to the iodine spin-orbit splitting. But depending on the net charge on the β-carbon atom, the internuclear distance where the crossing occurs may be altered. Our results indicate a higher curve-crossing probability (i.e., lower I* yield) for *n*-butyl iodide than

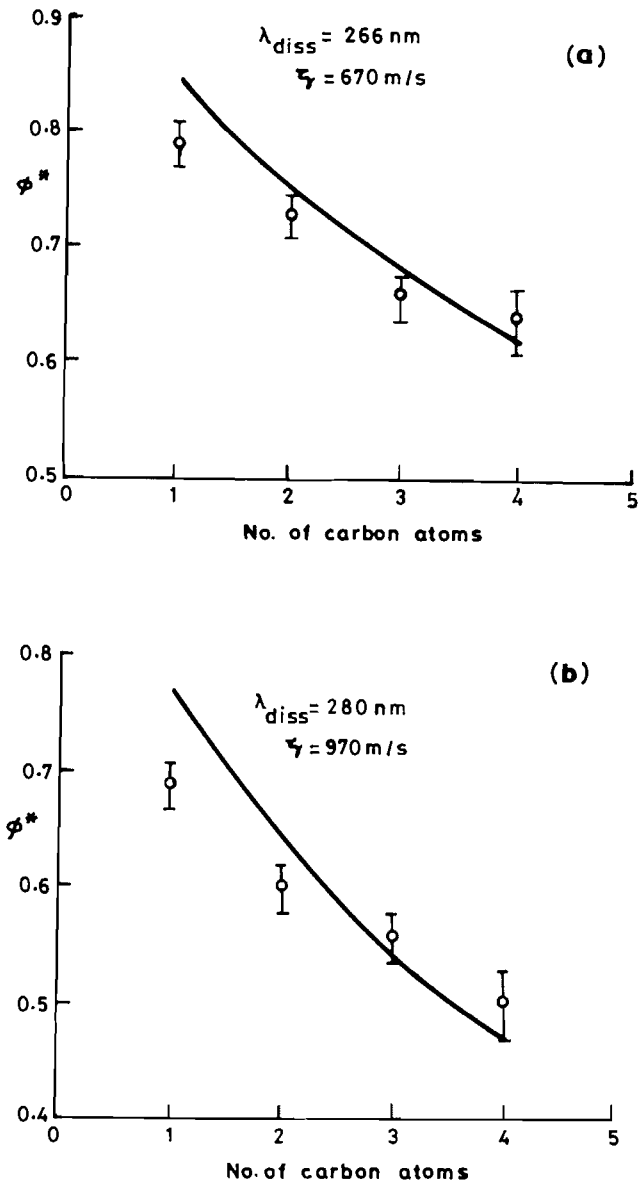

FIG. 4. I* quantum yields at (*a*) 266 nm, and (*b*) 280 nm as a function of number of carbon atoms in the alkyl radical. Solid lines are fits obtained from eq. [3] with ζ values shown on the respective curves.

for isobutyl iodide assuming similar crossing velocities for both.

Recently Guo and Schatz (21–23) carried out three-dimensional quantum mechanical calculations based on the fast Fourier transform method developed by Kosloff and Kosloff (24). Using the potential energy functions and the nonadiabatic coupling between the $^3Q_0$ and $^1Q_1$ states from Yabushita and Morokuma (25), they predicted the I* quantum yield as a function of dissociation wavelength. We have compared our experimental I* yields from CH_3I with Guo's (23) calculations (Fig. 5) and find that the trend is better reproduced when initial excitation is only to the $^3Q_0$ state. However, in his calculation the internal energy distribution in the methyl fragments is better reproduced when excitation to both $^3Q_0$ and $^1Q_1$ states is considered. We find that around 266 nm (near the absorption maxima of the *A* band) the I* yield reaches a maximum and drops much faster at longer wavelengths. The formation of I dominates at ≃305 nm, which is in apparent contradiction to the calculated results (23),

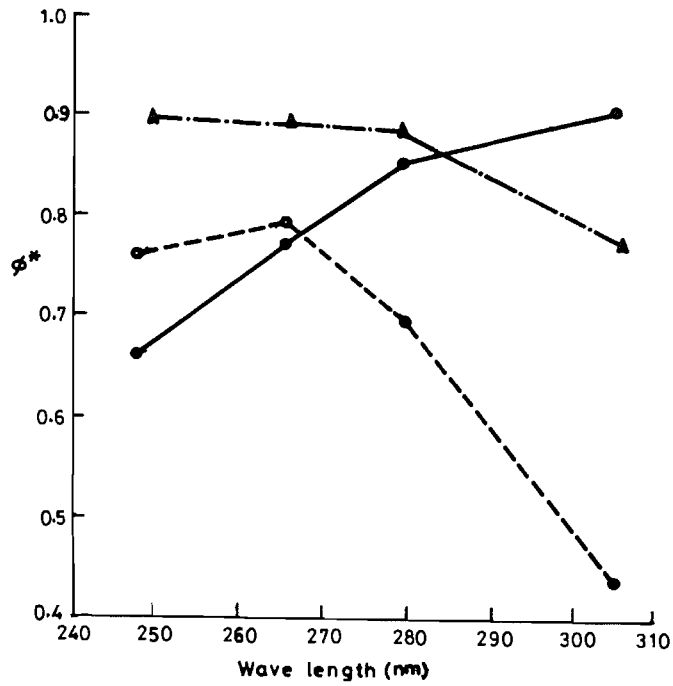

FIG. 5. Comparison of ϕ* obtained from a full three-dimensional quantum mechanical calculation (adapted from ref. 23) with initial excitation to the $^3Q_0$ state (dot-dash line), with initial excitation to both $^3Q_0$ and $^1Q_1$ states (solid line), and experiments (dotted line). The experimental ϕ* values at 248 nm are taken from ref. 8.

which predict a much higher I* yield at that wavelength. This discrepancy may be attributed to the fact that the contribution of the $^3Q_1$ state, which is important above 300 nm, has not been included in the above model. Insofar as the effects of substitution, size, and structure on the dynamics of primary alkyl iodide series in the ultraviolet are concerned, treatment by a full three-dimensional sophisticated model would be difficult and a semiclassical model with an accurate potential energy function might be an easier alternative to obtain a good dynamical picture for these molecules.

Conclusion

From the determination of the I* yields at ≃305-, 280-, and 266-nm dissociation of a series of alkyl iodides, it appears that the iodine atom in the spin-orbit excited state is the major product over the *A* band of alkyl iodides except near the red wing. Substantial contribution from the low-energy transition, $^3Q_1 \leftarrow N$, cannot be *undermined* at ≃300 nm absorption. Also, substitutions at the α- as well as the β-carbon atoms will alter the dynamics at the upper potential energy surfaces slightly.

Although a classical impulsive model is useful in describing the dynamics in one dimension, most of the details are lost in such a treatment. An appropriate full three-dimensional quantum mechanical model that contains contributions from all three excited states (i.e., $^1Q_1$, $^3Q_0$, and $^3Q_1$) may better explain the photodissociation dynamics in these molecules. What are more difficult to understand are the effects of substitution, size, and structure of the alkyl radicals on the coupling between the $^3Q_0$ and $^1Q_1$ states and the C—I distance where these two states cross. We hope that future work in this direction will better answer some of these questions.

Acknowledgements

We would like to thank Mr. P.V. Ramakrishnan for designing

the pulse divider–delay generator circuit for us. Generous financial support from the Director, Indian Institute of Science, the Department of Science & Technology, Govt. of India, and the Department of Atomic Energy, Govt. of India, for this project is gratefully acknowledged.

1. A. Gedanken and M.D. Rowe. Chem. Phys. Lett. **34**, 39 (1975).
2. S.J. Riley and K.R. Wilson. Faraday Discuss. Chem. Soc. **53**, 132 (1972).
3. M. Dzvonik, S. Yang, and R. Bersohn. J. Chem. Phys. **61**, 4408 (1974).
4. R.K. Sparks, K. Shobatake, L.R. Carlson, and Y.T. Lee. J. Chem. Phys. **75**, 3838 (1981).
5. H.W. Herman and S.R. Leone. J. Chem. Phys. **76**, 4766 (1982).
6. M. Shapiro and R. Bersohn. J. Chem. Phys. **73**, 3810 (1980).
7. G.N.A. van Veen, T. Baller, A.E. de Vries, and N.J.A. van Veen. Chem. Phys. **87**, 405 (1984).
8. P. Brewer, P. Das, G. Ondrey, and R. Bersohn. J. Chem. Phys. **79**, 720 (1983).
9. M.D. Barry and P.A. Gorry. Mol. Phys. **52**, 461 (1984).
10. F.G. Godwin, P.A. Gorry, P.M. Hughes, D. Raybone, T.M. Watkinson, and J.C. Whitehead. Chem. Phys. Lett. **135**, 163 (1987).
11. W.P. Hess, S.J. Kohler, H.K. Haugen, and S.R. Leone. J. Chem. Phys. **84**, 2143 (1986).
12. S.M. Penn, C.C. Hayden, K.J.C. Muyskens, and F.F. Crim. J. Chem. Phys. **89**, 2909 (1988).
13. R. Ogorzalek Loo, H.P. Haerri, G.E. Hall, and P.L. Houston. J. Chem. Phys. **90**, 4222 (1989).
14. K.Q. Lao, M.D. Person, P. Xayariboun, and L.J. Butler. J. Chem. Phys. **92**, 823 (1990).
15. T.F. Hunter and K.S. Kristjansson. Chem. Phys. Lett. **58**, 291 (1978).
16. D.W. Chandler, J.W. Thoman, Jr., M.H.M. Janssen, and D.H. Parker. Chem. Phys. Lett. **156**, 151 (1989).
17. S. Uma and P.K. Das. Curr. Sci. **65**, 307 (1993).
18. R.S. Mulliken. Phys. Rev. **50**, 1017 (1936).
19. H.J. Hwang and M.A. El-Sayed. J. Chem. Phys. **94**, 4877 (1991).
20. H.J. Hwang and M.A. El-Sayed. J. Phys. Chem. **96**, 8728 (1992).
21. H. Guo and G.C. Schatz. J. Chem. Phys. **93**, 393 (1990).
22. H. Guo. J. Chem. Phys. **96**, 2731 (1992).
23. H. Guo. J. Chem. Phys. **96**, 6629 (1992).
24. D. Kosloff and R. Kosloff. J. Comput. Phys. **52**, 35 (1983).
25. S. Yabushita and K. Morokuma. Chem. Phys. Lett. **153**, 3130 (1988).